CHAPTER-VIII

AN INSENSITIVE LINEAR SINGLE-ELEMENT-CONTROL PULSE GENERATOR

8.1 INTRODUCTION

Generation of harmonic to relaxation oscillation using the non-linearity of the antisymmetric self saturating transfer characteristics (ASTC) of an emitter coupled differential pair (ECDP) has been presented[1] in Chapter-VII. The ASTC had been approximated by a transcendental function of hyperbolic tangent type resulting in a two parameter non-linear differential equation and the mode of oscillation could be adjusted by the control of these two parameters. The two parameter control could be effected by changing the capacitor ratios or the resistance ratios in the frequency determining network or by changing the operating slope ab of the ASTC. Interestingly, the operating slope ab can be changed by bias voltage change of the ECDP and this was utilised to obtain a VCO[2] giving sinusoidal output. This has also been presented in Chapter-VII. However, the frequency range obtained was not very large. In practice, however, wide frequency-deviation ratio oscillators, basically, are of multivibrator type, providing pulse or square wave output. Using the ASTC of the proposed ECDP a linear wide range, variable frequency pulse generator can be designed. This pulse generator can be conveniently adapted to instrumentation system with the control element replaced by a suitable transducer to provide a process parameter to pulse period conversion facility.

Since no closed form solution of the two-parameter non-linear differential equation with a transcendental function is possible, an approximate analytical approach, to enumerate the design criteria and predict the behaviour of such a system in relaxation mode, to obtaining symmetric pulse waveform, has been presented in this chapter[3*]. The repetition rate of the generated pulse wave form is obtained through jump behaviour[4], while hyberbolic tangent non-linear characteristic[1] is used to obtain the shift in the operating point thereby correcting the repetition rate of the generator. The number of frequency determining parameters in such a system is reduced to a minimum with the provision for linearly varying the time period with a single resistive element.

The validity of the analytical approach has been tested experimentally and the repetition rate and the region of linearity of the controlled generator have been found to agree closely with the theoretical analysis. Conditions have also been derived under which the frequency sensitivity of the circuit can be minimized. The effects of temperature on both the active and passive parameters have been considered and it has been indicated how the effect of temperature on the frequency determining parameters may be utilized for compensation, offering a scope of improvement which may be best exploited in integrated circuit implementation of such generators.

Experimental results, covering several aspects of the proposed circuit with discrete components, for substantiating the theoretical analysis, are shown in tables and a graph.

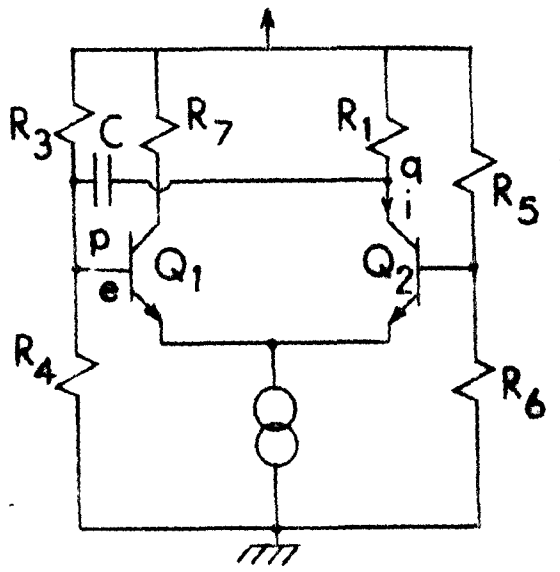

Fig.8.1 Circuit of the propsed generator

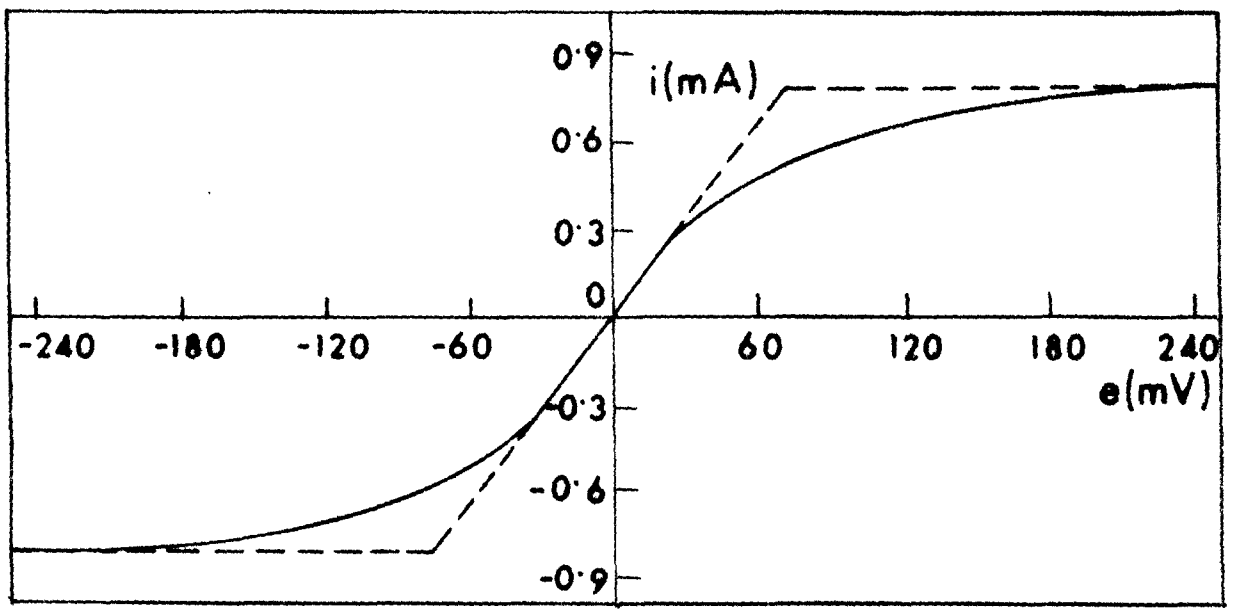

Fig.8.2 The normalized transfer characteristic of the ECDP

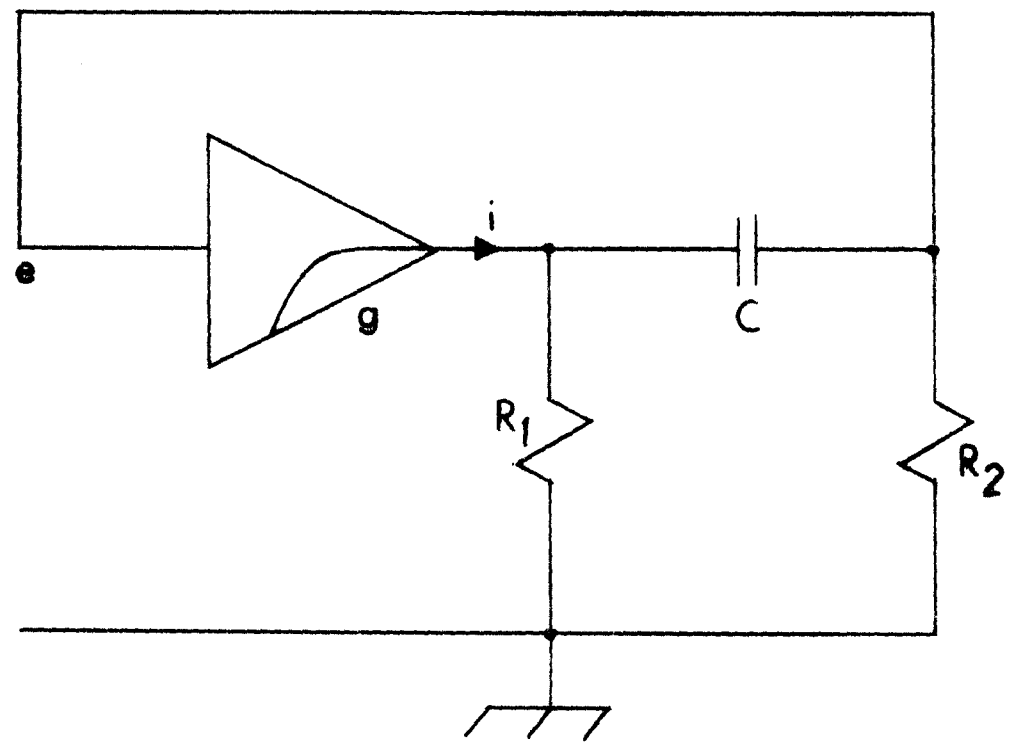

Fig. 8.3 Equivalent scheme of Fig. 8.1 .

8.2 THE SCHEME AND FREQUENCY OF OSCILLATION

The scheme of the proposed circuit is shown in figure 8.1. While the capacitor is open R_3, R_4, R_5 and R_6 are adjusted for balanced biasing and the differential pair acts as a transconductance element between the points 'p' and 'q' whose saturation transfer characteristic is shown in figure 8.2 and is assumed to be represented by the transcendental form[1]

$$i = a \tanh be \tag{8.1}$$

when the feedback path is closed through the capacitor, the positive feedback provided sets relaxation oscillation in the circuit which can be easily deduced from the equivalent circuit of figure 8.1 drawn in figure 8.3 where R_2 is $R_3 \parallel R_4$. The system differential equation[1]

$$CR_1R_2 \frac{de}{dt} \left[\left(\frac{1}{R_1} + \frac{1}{R_2} \right) - \frac{di}{de} \right] + e = 0 \tag{8.2}$$

represents the dynamic model of the oscillator. Considering the linearized saturation characteristic as shown by the dotted lines in figure 8.2 whose slope at the operating point is g and the fact that a jump would occur in the system voltage to double its value on just reaching the saturation level (because the coupling is by capacitor C only), one can obtain the repetition rate by integration of equation (8.2)[4] as

$$T = C(R_1 + R_2) \ln (2gR_1 - 1) \tag{8.3}$$

If R_1 is controlled for governing the repetition rate, while the operating point remains fixed, both the product terms vary

simultaneously giving a large variation in the repetition rate. The normalized rate of this is in fact given by

$$\rho = \frac{1}{C}\frac{dT}{dR_1} = \frac{2g(R_1 + R_2)}{2g\,R_1 - 1} + \ln\,(2gR_1 - 1) \qquad (8.4)$$

which is much larger than that in conventional design.

For linearity of the T-R_1 relationship, $\ln\,(2gR_1 - 1)$ should not vary substantially with R_1. However, from equation (8.4), a range of values for R_1 can be obtained for which this is approximately true and an almost linear variation of T with respect to R_1 over this range is obtainable.

Differentiating equation (8.4) with respect to R_1

$$\frac{d\rho}{dR_1} = \frac{4g}{(2gR_1 - 1)^2}\left[g\,(R_1 - R_2) - 1\right] \qquad (8.5)$$

one observes that a near linear T-R_1 relationship is obtained for

$$g(R_1 - R_2) = 1 \qquad (8.6a)$$

From equation (3) one finds that the oscillation condition requires

$$R_1 \rangle \frac{1}{2g} \qquad (8.6b)$$

Showing compatibility of equation (8.6).

For a given value of R_2, therefore, a range of values for R_1 is to be chosen following equations (8.6a) and (8.6b) such that ρ is nearly constant over that range. Deviation from linearity at

any value of T can be obtained from equations (8.4) and (8.6a) for the corresponding value $R_1 = R_{1x}$ (say)

$$\delta_L = \frac{\rho_x - \rho_o}{\rho_o} = \frac{1}{2 + \ln(2gR_2 + 1)} \left[\frac{2g(R_2 - R_{1x}) + 2}{2GR_{1x} - 1} + \ln \left(\frac{2gR_{1x} - 1}{2gR_2 + 1} \right) \right] \qquad (8.7)$$

where ρ_o is obtained by substituting equation (8.6a) in equation (8.4). For allowable δ_L, the limiting values of R_{1x} can now be evaluated from equation (8.7).

8.3 THE OPERATING POINT AND VALUE OF g

The value of g is obtained from the actual plot[1] for balanced bias conditions with compatible values of R_j's, j = 1,3,4,5,6 as dictated by equation (8.6b) and for better linearity in $T-R_1$, also by equation (8.6a). However, as oscillation sets in, the operating point of the transistor Q_1 (figure 8.1) shifts, thereby changing the value of g. This shift in the point is only graphically obtainable through complex analysis[5] for an arbitrary mode of oscillation. As only relaxation oscillation is considered here, this shift is maximum and is calculable from the non-linear saturation transfer characteristic. When shift occurs, the approximated linearized characteristic changes such that the slope g is also different. In fact this increases the value of g, as the constant current source (CCS) at the emitters decreases the saturation voltage in the ASTC of the differential pair, when the idealized and linearized model of this is considered. At hard relaxation the input e

(figure 8.1) via the base-emitter junction reduces the effective saturation voltage to half its balanced bias condition. Therefore, from equation (8.1) the effective value of g is calculated

$$g_e = g \cosh^2 be = g \cosh^2(0.5) = 1.27g \qquad (8.8)$$

This value of g_e is used in equation (8.3) for calculating the repetition rate as R_1 is controlled. As relaxation through jump phenomenon occurs, the waveform at the output point q is not a square-wave. The waveform undergoes a certain change, retaining however the pulse nature, because of the difference in voltage across Q_2 and R_1. The output waveform becomes nearly square when these voltages are very close. A square-wave can, however, easily be extracted by standard clipping techniques.

8.4 EFFECT OF NON-IDEAL CURRENT SOURCE

When the current source at the emitters is replaced by a simple resistor R_{EE} of correct value, the basic operation of the generator remains unaltered, but there is a marginal shift in the controlled frequency range. This occurs because the 'non-ideal' current source tends to shift the operating point in a different manner, producing a different linearized slope g_f, however close its value may be to g_e. In the balanced biased condition in this case, let I_{EQ} denote the balanced emitter operating currents on each side. In hard relaxation oscillation let this value be I_{ES}. Let E_{OB} be the amplitude of base drive at p (figure 8.1) due to this oscillation, then one can write the approximate equation during oscillation for transistor Q_1 as,

$$I_{ES} = I_{EQ} + \frac{E_{OB} - 2R_{EE}\,(I_{ES} - I_{EQ})}{h_{IE}}\,h_{FE} \qquad (8.9)$$

where h_{IE} and h_{FE} have the usual significances. Equation (8.9) is simplified to

$$I_{ES} = I_{EQ}\left[1 + \frac{E_{OB}}{I_{EQ}\left(\frac{h_{IE}}{h_{FE}} + 2R_{EE}\right)}\right] \qquad (8.10)$$

showing an increase in the saturation current. In fact when relaxation oscillation occurs, the amplitude at the base is fixed by the non-linearity of the slope of the characteristic and actual saturation occurs at a higher value of e, say E_{BSS}, but this apparently does not change the saturation current, I_{ESO}(say). The oscillation amplitude would, however, cause a change in the actual emitter current for the changed slope that occurs because of the shift in the operating point. This is calculated in equation (8.10) where E_{OB} is to be replaced by E_{BSS}, which in turn is calculated from equation (8.1) by assuming a linearized and idealized model of the enhanced-slope saturation characteristic with tanh be = 1, as saturation current is assumed constant. This gives

$$E_{OB} = E_{BSS} = \frac{1}{b}\tanh^{-1} 1 = E_{BSO}\tanh^{-1} 1 \qquad (8.11)$$

The parameter b is obtained from the standard saturation model. From equations (8.10) and (8.11) I_{ES} is calculated and used to obtain

$$g_f = \frac{I_{ES}}{E_{BSO}} \qquad (8.12)$$

which is the new value of g with the non-ideal constant current generator.

8.5 SENSITIVITY TO SUPPLY, TEMPERATURE AND PASSIVE PARAMETERS

It would be observed from equation (8.3) that in the proposed oscillator, the frequency changes when g is affected. As g is basically dependent on the emitter current, when an ideal constant current source supplies the emitters of the differential pair, g is not affected. Even when the supply voltage changes within prescribed limits, the current remains unaltered, and once relaxation oscillation sets in, g_e would not change its value from the one calculated from equation (8.8).

If however the 'approximate current source' obtained with a resistor between common emitters and ground is considered, I_{EE} would change as the supply voltage is varied. This can easily be seen from equations (8.9) and (8.10). In fact, if one assumes h_{IE} and h_{FE} do not change to the extent to warrant any consideration, I_{ES} changes directly with I_{EQ} as the supply changes. From equation (8.10) it can further be shown that if the supply varies by $\pm \triangle E_s$, $\pm \triangle I_{EQ}$ is given by

$$\pm \triangle I_{EQ} = \pm \frac{K \triangle E_s}{2R_{EE}} \qquad (8.13)$$

where K is a constant determined by the biasing chain. Frequency variation due to supply change is therefore dependent on K and R_{EE}. For CCS, $R_{EE} \rightarrow \infty$ giving no variation in frequency due to supply fluctuation. Table-8.1 gives these results both with ideal and non-ideal CCS for a $\pm$ 10% supply variation.

TABLE-8.1

EXPERIMENTAL SENSITIVITY FIGURES TO SUPPLY VARIATION

$\frac{\Delta E_s}{E_s}$ (%)	$\frac{\Delta T}{T} \times 100$ (%), with CCS	$\frac{\Delta T}{T} \times 100$ (%), with R_{EE}
- 10.0	- 0.440	- 5.60
- 7.5	- 0.300	- 4.20
- 5.0	- 0.200	- 2.80
- 2.5	- 0.100	- 1.40
0	0	0
2.5	0.095	1.50
5.0	0.180	2.70
7.5	0.280	4.20
10.0	0.390	5.50

Frequency shift due to temperature variation is more serious, particularly with the CCS design when the CCS is not individually compensated. The differential pair is self-compensated as regards temperature[6] but this degree of compensation is also important. A shift in the value of g occurs because of the bias unbalance resulting due to inequality in the temperature coefficient of V_{BE} of the pair. As the differential temperature coefficient is likely to be small for a matched pair mounted in the same header g varies almost linearly with it. From equation (8.3) neglecting higher order products of the differential quantities, one can easily derive the change in the repetition rate with changes in resistances, capacitances and the transconductance with temperature as

$$\frac{\Delta T}{T} = \frac{\Delta C}{C} + \frac{\Delta R}{R} + \frac{\ln\left[1 + (\Delta g/g) + (\Delta R/R)\right]}{\ln(2g\,R_1 - 1)} \qquad (8.14)$$

Where it has been assumed that

$$\frac{\Delta R_1}{R_1} = \frac{\Delta R_2}{R_2} = \frac{\Delta R}{R}$$

As can be seen from equation (8.14) $\Delta T/T$ can be made zero, if either

$$\frac{\Delta C}{C} = \frac{\Delta R}{R} = \frac{\Delta g}{g} = 0 \qquad (8.15a)$$

or

$$\frac{\Delta R}{R} = -\frac{\Delta C}{C} = -\frac{\Delta g}{g} \qquad (8.15b)$$

While equation (7.15a) is a little hypothetical, equation (8.15b) is more easily satisfied in practice particularly in integrated circuit forms. Actual values of $\Delta T/T$ would depend on the magnitudes and signs of $\Delta C/C$, $\Delta R/R$ and $\Delta g/g$, and thus a third probable alternative for $\Delta T/T = 0$ is

$$\frac{\Delta C}{C} + \frac{\Delta R}{R} = -\frac{\ln\left[1 + (\Delta g/g) + (\Delta R/R)\right]}{\ln\,(2gR_1 - 1)} \qquad (8.15c)$$

The wrost-case shift in T with the change in temperature is studied for the proposed circuit and it is shown that even when adequate compensation is not provided the change in repetition rate is within tolerable limits.

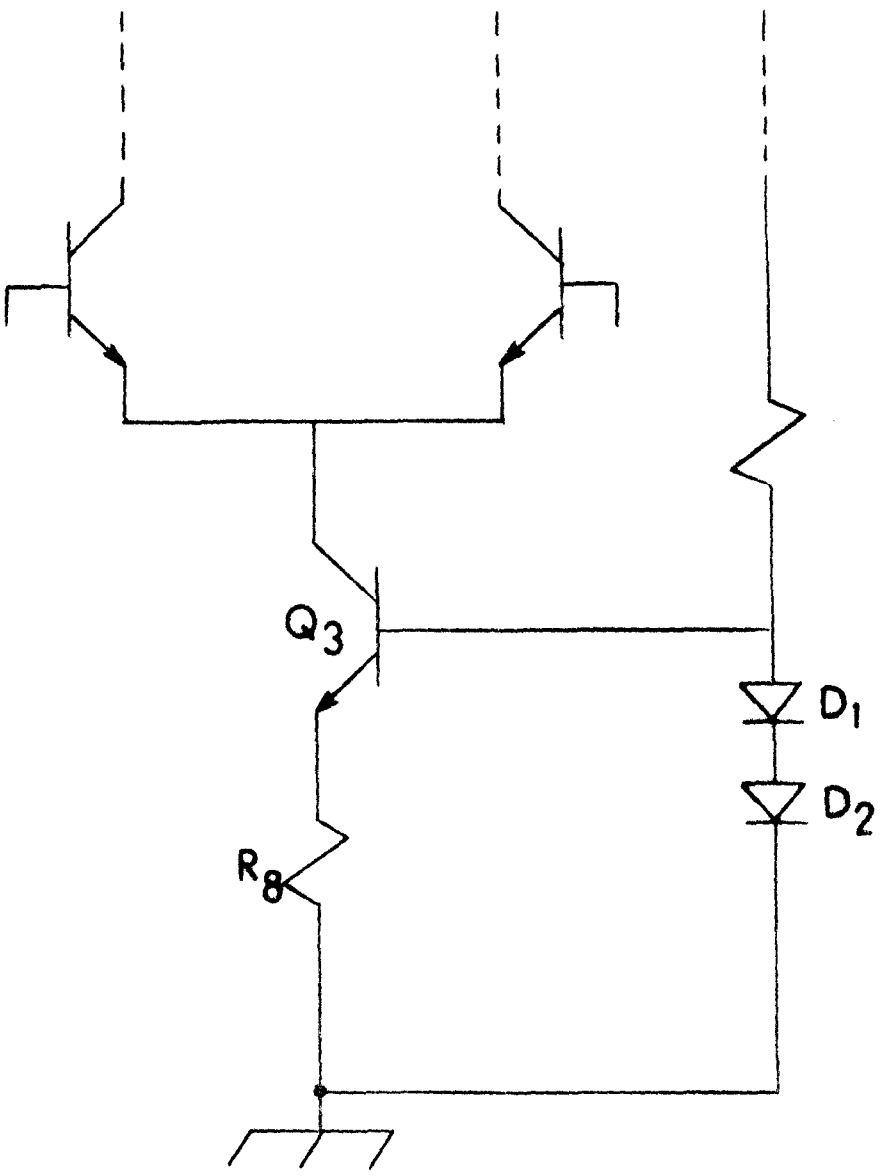

Fig. 8.4 Scheme of the CCS

The circuit of the CCS used is shown in figure 8.4. The temperature coefficient of the base-emitter junction diode of transistor Q_3 being equal to the temperature coefficient of the biasing diodes. With the rise in temperature, the base driving potential would decrease as the biasing chain contains two diodes, thus decreasing the transistor current and making $\Delta g/g$ negative. Since the change in the transistor current is linearly related to its base potential and the temperature coefficient of the diode is large, as shown subsequently, one derives

$$\left|\frac{\Delta g}{g}\right| > \left|\frac{\Delta R}{R}\right|$$

such that the last term in equation (8.14) is actually negative. The approximate value of $\Delta g/g$ can be calculated from the diode temperature coefficient ($\Delta E_d/°C$) and the temperature coefficient of the input offset voltage of the differential pair ($\Delta E_p/°C$).

The approximate relation is

$$\frac{\Delta g}{g} \approx \pm \frac{|\Delta E_p|}{E_{BB} \pm |\Delta E_p|} - \frac{|\Delta E_d|}{I_{EQ} R_e} \qquad (8.16)$$

Typical values of $|\Delta E_p|$ and $|\Delta E_d|$ are 6 μV/°C and 2.5 mV/°C respectively and for the proposed circuit E_{BB} = 2.117V, $I_{EQ} = 0.77 \times 10^{-3}$A, and R_e = 390 ohms, from which one can easily show that $|\Delta E_p| / (E_{BB} \pm |\Delta E_p|) \ll \Delta E_d / I_{EQ} R_e$ such that, one can always write

$$\frac{\Delta g}{g} = -\frac{|\Delta E_d|}{I_{EQ} R_e}$$

Further $(\Delta R/R)/°C = 50$ p.p.m. and $(\Delta C/C)/°C = -150$ p.p.m. and using the above data $\Delta T/T$ can be calculated from equation (8.14).

If however, a non-ideal current source is considered the last term on the right-hand side of equation (8.16) is replaced by $\Delta R/R$ such that

$$\frac{\Delta g}{g} \approx \pm \frac{|\Delta E_p|}{E_{BB} \pm |\Delta E_p|} - \frac{\Delta R}{R} \qquad (8.17)$$

Evidently

$$\left|\frac{\Delta R}{R}\right| < \left|\frac{\Delta E_d}{I_{EQ} R_e}\right| \qquad (8.18)$$

so that, in general it is true that

$$\left|\frac{\Delta T}{T}\right|_{CCS} > \left|\frac{\Delta T}{T}\right|_{R_{EE}} \qquad (8.19)$$

Experimental results confirming the above are shown in Table-8.2. Equations (8.14) - (8.17) also confirm that it is possible to reduce the temperature sensitivity of T to a minimum by correct component choice and appropriate design of the CCS, and as such, temperature sensitivity should not pose any problem for the generator.

TABLE-8.2

TEMPERATURE SENSITIVITY; NOMINAL TEMPERATURE 30°C

Δt (°C)	$\frac{\Delta T}{T}$ with CCS, x 10^{-3}		$\frac{\Delta T}{T}$ with R_{EE}, x 10^{-3}	
	Theoretical	Experimental	Theoretical	Experimental
- 10	21.22	19.20	0.993	1.071
- 5	10.79	9.00	0.496	0.583
0	0	0	0	0
5	-11.36	- 9.20	-0.504	-0.620
10	-22.96	-19.90	-1.007	-1.980
15	-35.20	-28.70	-1.511	-2.330
20	-47.98	-39.80	-2.015	-2.850
25	-61.40	-47.70	-2.517	-3.420

One should also see how the repetition rate changes with the tolerance limits of the passive parameters R_1, R_2 and C. Using the definition of classical sensitivity one gets from equation (8.3).

$$S^T = \sum_{i=1,2} S_{Ri}^T = S_C^T = 2 + \frac{2gR_1}{(2gR_1-1)\ln(2gR_1-1)} \qquad (8.20)$$

Since $2gR_1 \gg 1$, S^T never tends to be very large.

8.6 RESULTS AND DISCUSSION

The circuit was tested with both a constant current source and a fixed emitter resistor R_{EE} = 1k ohm and with C = 0.06 μF, R_2 = 1.308k ohms. The experimental results with CCS are shown along with the theoretical curves, in figure 8.5. Results are seen to be

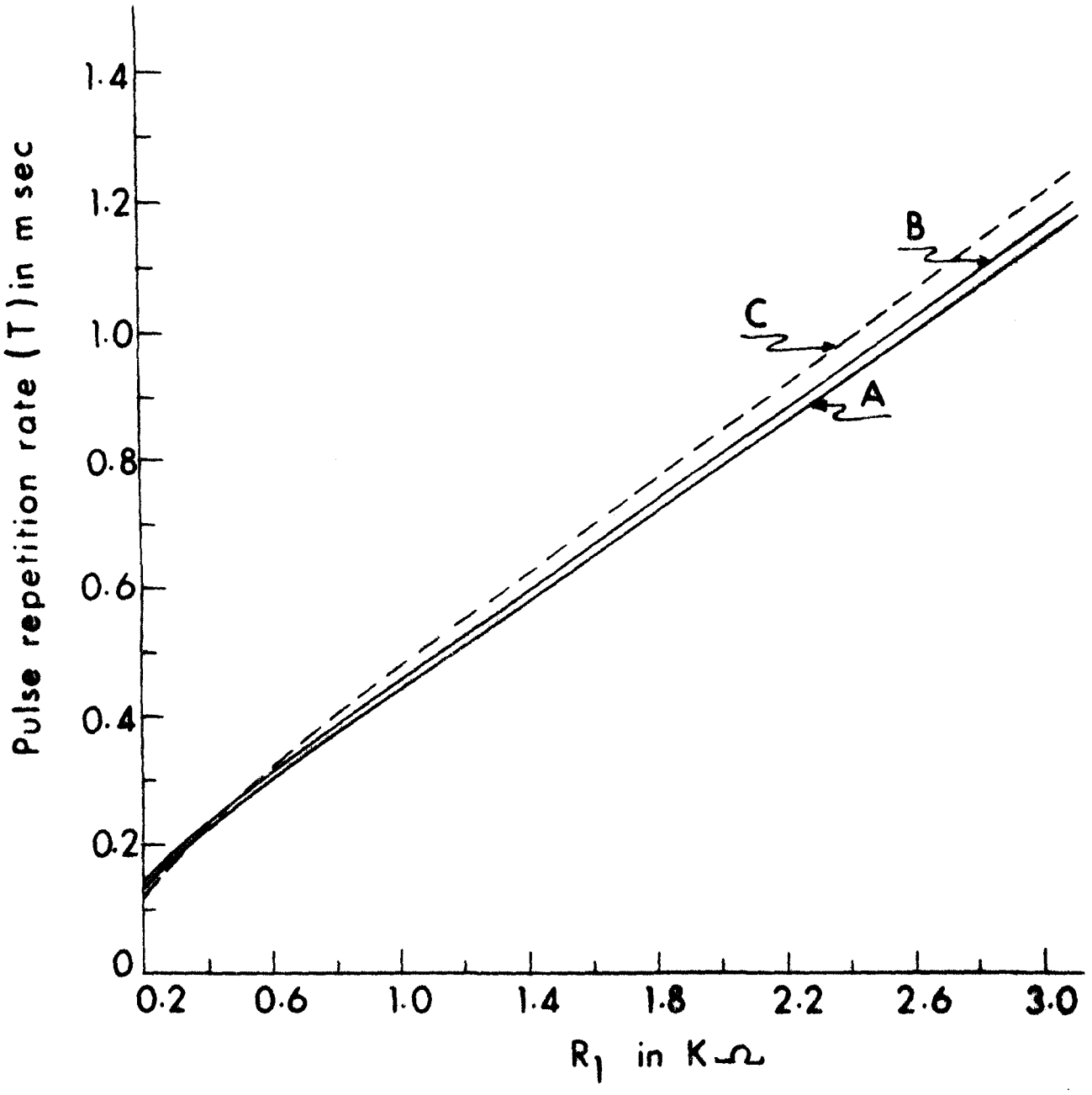

Fig.8.5. R_1 – T plot of the generator; R_2 = 1.308 KΩ, C = 0.06 μF

Curve A: Calculated with CCS (g_e = 13.06 m ℧)

Curve B: Calculated with R_{EE} (g_f = 14.4 m ℧)

Curve C: Experimental with CCS

quite in agreement with the analysis. The results with a simple resistor have not been shown in figure 8.5 as they are almost coincident with those using the CCS. In both theoretical and experimental results, except for a small region of low R_1 the T-R_1 relationship is found to be almost linear. Using equation (8.7) it can be shown that the linearity of repetition rate is within $\pm$ 5% for a range of 0.36 ms to 1.12 ms, when R is varied from 750 ohms to 3k ohms. From figure 8.5, the practical figure for linearity is seen to be nearly the same in this range of R_1. However, if larger non-linearity is tolerable the range can be extended further.

For varying supply voltage the shifts in the repetition rate from a nominal value of 0.833 ms are shown in Table-8.1 for both cases. While the percentage variation obtained with the CCS is less than 0.45%, that with a simple resistor is as high as 5.6% when the supply is varied within $\pm$ 10%.

The theoretical and practical data for temperature sensitivity of the repetition rate at its nominal value of T_o = 0.833 ms are given in Table-8.2 with the CCS and R_{EE}. As predicted, this sensitivity is larger with the CCS. For a 25°C increase in temperature, T_o is shown to shift by about 6.14% with the CCS, while with R_{EE} the change is only about 0.3%. It is interesting to note that practical $\Delta T/Ts$ with the, CCS are less than the calculated values, while with R_{EE} the nature of the variation is the opposite. However, in both cases results are quite confirmatory. The discrepancy may be attributed to the fixed idealized data assumed in the calculations.

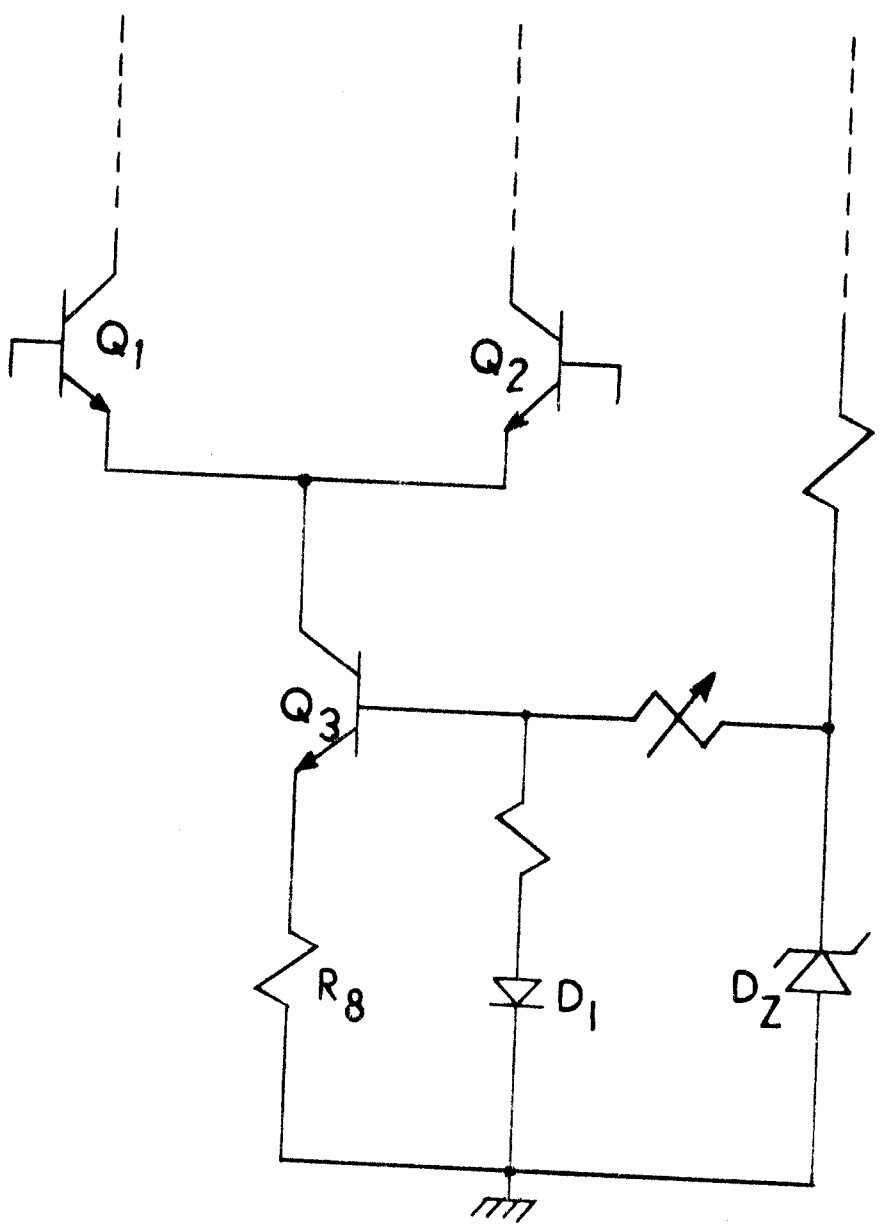

Fig.8.6 Circuit scheme of the compensated CCS

The temperature sensitivity is considerably improved with the CCS feeding the differential pair, if the CCS is individually compensated. A scheme of such a compensated CCS is shown figure 8.6. The Zener diode D_Z should have a zero temperature coefficient. The base drive potential here does not change with temperature as the variation in V_{EB} of the transistor Q_3 would tend to be compensated by an opposite change in diode D_1 voltage drop. Table-8.3 shows the theoretical and experimental sensitivity of time period with temperature.

TABLE-8.3

TEMPERATURE SENSITIVITY OF TIME PERIOD WITH A COMPENSATED CCS FEEDING THE DIFFERENTIAL PAIR; NOMINAL TEMPERATURE 30°C

Δt (°C)	$\frac{\Delta T}{T} \times 10^{-3}$	
	Theoretical	Experimental
- 10	0.993	1.00
- 5	0.496	0.46
0	0	0
5	-0.504	-0.57
10	-1.007	-1.37
15	-1.511	-1.80
20	-2.015	-2.37
25	-2.517	-2.93

The above results have been obtained using discrete components and a matched pair of transistors.

It may be shown that the contribution of the last term of equation (8.14) is negligible for the case when the coupled emitter is fed from a compensated CCS and the temperature sensitivity of the time period is predominantly dependent on the temperature coefficients of the passive parameters. Hence the temperature sensitivity of a fixed-frequency pulse generator can be made to approach zero by adopting hybrid integration techniques, where the passive components should be of the thin-film type[7].

However for a variable time period symmetric pulse generator, two of the frequency-determining elements R_1 and C [equation (8.3)] are externally controlled and the rest of the circuit may be integrated. In such a case the expression for the temperature sensitivity of T is obtained from equation (8.3), neglecting the higher order products of the differential quantities, as

$$\frac{\Delta T}{T} = \frac{\Delta C}{C} + \frac{\Delta R_1}{R_1 + R_2} + \frac{\Delta R_2}{R_1 + R_2} + \frac{\ln(1+(\Delta g/g)+(\Delta R_1/R_1)}{\ln(2gR_1 - 1)} \qquad (8.21)$$

In equation (8.21) the contribution due to the last term is still negligible such that equation (8.21) reduces to

$$\frac{\Delta T}{R} = \frac{\Delta C}{C} + \frac{\Delta R_1}{R_1 + R_2} + \frac{\Delta R_2}{R_1 + R_2} \qquad (8.22)$$

If, now, the frequency-determining passive elements are appropriately chosen ($\Delta R_1/R_1$ = + 100 p.p.m./°C, e.g. Nichrome potentiometer; $\Delta R_2/R_2$ = - 100 p.p.m./°C, thin-film integrated), $\Delta T/T$ is

easily shown to be essentially dependent on the thermal drift of the capacitor alone. If a high quality ceramic chip capacitor with a temperature coefficient of NPO ± 30 p.p.m./°C is used[7], the temperature sensitivity of the time period would tend to be of the same order, which is about one order lower than that obtained with discrete component design.

8.7 CONCLUSION

A pulse generator scheme with a single emitter-coupled differential transistor pair was studied and by means of an analytical approach it has been shown that by using a temperature-compensated constant current source feeding the coupled emitters, the generator can produce very stable oscillation. Experimental stability figures of ± 0.44% for ± 10% supply voltage change and less than 150 p.p.m./°C with temperature variation are easily obtained in the scheme. Conditions for further improving these figures, particularly the temperature sensitivity, have been obtained when this configuration is adopted in an integrated circuit, as can be seen from equation (8.22). Besides, the repetition rate has been shown to be linearly varying with a single resistive element and the experimental figures actually show a linear variation of ± 55% around 0.65 ms for a resistance variation of ± 62% around 1.6k ohms.

REFERENCES

1. Roy,S.B. and Patranabis,D. : 'Non-linear oscillations using antisymmetric transfer characteristics of a differential pair'; Int. J. Electron., Vol.42, No.1, pp.19-32, 1977.

2. Roy,S.B. and Patranabis,D. : 'Voltage-controlled oscillator using an emitter-coupled differential pair'; Electron. Lett., Vol.13, No.19, pp.590-591, Sept.1977.

*3. Roy,S.B. Patranabis,D. and Kundu,P. : 'An insensitive linear single-element-control pulse generator'; Int. J.Electron, Vol.46, No.3, pp.229-239, 1979.

4. Sen,P.C. and Patranabis,D. : 'Oscillations in a first order all-pass filter'; Int. J. Electron, Vol.29, No.1, pp.83-91, 1970.

5. Clarke,K.K. : 'Design of self-limiting transistor sinewave oscillator'; IEEE Trans. Circuit Theory, Vol.CT-13, No.1, pp.58-63, March 1966.

6. Kundu,P. and Roy,S.B. : 'A temperature-stable RC transistor oscillator'; Proc.IEEE, Vol.57, No.3, pp.356-357, March 1969.

7. Moschytz,G.S. : 'Linear Integrated Networks : Fundamental'; New York : Van Nostrand Reinhold, 1974, pp.367-407.

---

* Chapter-VIII is based mainly on this publication.